

Shape coexistence and high- K states in ^{74}Se populated following the β decay of ^{74}Br

E. A. McCutchan,^{1,2} C. J. Lister,^{1,3} T. Ahn,⁴ V. Anagnostatou,^{4,5} N. Cooper,⁴ M. Elvers,^{4,6} P. Goddard,^{4,5} A. Heinz,⁴ G. Ilie,^{4,7} D. Radeck,^{4,6} D. Savran,^{4,8} and V. Werner⁴

¹Physics Division, Argonne National Laboratory, Argonne, Illinois 60439, USA

²National Nuclear Data Center, Brookhaven National Laboratory, Upton, New York 11973, USA

³Department of Physics and Applied Physics, University of Massachusetts Lowell, Lowell, Massachusetts 01854, USA

⁴Wright Nuclear Structure Laboratory, Yale University, New Haven, Connecticut 06520, USA

⁵Department of Nuclear Physics, University of Surrey, Guildford GU2 7XH, United Kingdom

⁶Institut für Kernphysik, Universität zu Köln, DE-50937 Köln, Germany

⁷National Institute for Physics and Nuclear Engineering, P. O. Box MG-6 Bucharest-Magurele, Romania

⁸ExtreMe Matter Institute EMMI and Research Division, GSI, Helmholtzzentrum, Darmstadt, Germany

(Received 19 October 2012; revised manuscript received 7 December 2012; published 8 January 2013)

Excited states in ^{74}Se were populated following the ϵ/β^+ decay of ^{74}Br , mainly from the $J = K = 4$, 13.8-keV β -decaying isomer. Off-beam γ -ray spectroscopy was performed with the array of Clover HPGe detectors at WNSL Yale. Many new transitions were observed and rigorous spin assignments were made based on γ - γ angular correlations. The β -decay strength was found to proceed almost entirely to a few high-lying states near 4500 keV, which are consistent with deformed two-quasineutron high- K configurations. These doorway states then provide an effective tool for populating and identifying the lower prolate structures. Once categorized, the low-lying states of ^{74}Se can be described as a set of near-spherical vibrational levels mixing strongly with a spectrum of prolate states which have an unperturbed bandhead near 1350 keV.

DOI: [10.1103/PhysRevC.87.014307](https://doi.org/10.1103/PhysRevC.87.014307)

PACS number(s): 21.10.Re, 23.20.Lv, 27.50.+e

I. INTRODUCTION

Shape coexistence of one kind or another has been an obsession for spectroscopists throughout the era of big γ -ray arrays. Some manifestations are very clear, like superdeformation [1] and fission isomers [2] in heavy nuclei and the so-called “island of inversion” [3] in lighter systems. The attraction is compelling; for experimentalists there are clear observables which can quantify the shapes and the degree of mixing, while for theoreticians there are the challenges of balancing shape-driving single-particle effects against the collective correlations which cause pairing and deformation.

In middle mass nuclei with $N \sim Z$, the nuclei in the Se-Br-Kr region are now well known [4–6] to display a variety of shapes, some of which are very collective and highly deformed. However, the barriers between the competing shapes are often quite low, especially at low spin, so there is considerable mixing of wave functions and the very notion of the lowest states having simple shapes is often misconceived. The Hartree-Fock-like calculations of Petrovici [7], Bender [8], and Girod [9] have clearly demonstrated these issues. Nonetheless, careful and detailed studies of middle mass nuclei, aimed at rather complete spectroscopy of all the low-lying states, can lead to unfolding the configuration mixing and revealing the topology of the binding-energy landscape, including the most bound shapes and the barriers between them.

There have been many interpretations of the structure of ^{74}Se . Initial studies [10,11] proposed the ground state to be a spherical structure coexisting with a deformed rotational band built on the low-lying first excited 0^+ state. Both Adam *et al.* [12] and Radhi and Stewart [13] calculated ^{74}Se in the framework of the interacting boson model (IBM) and found they could reproduce the experimental spectrum using just a

vibrational-like structure with no need to introduce a shape coexistence interpretation. Similarly, ^{74}Se and its neighbors have been successfully described by the supersymmetry scheme in the vibrational limit [14]. A more recent high-spin study proposed [15] new spin assignments in ^{74}Se which changed the prior interpretation of the so-called γ band into a deformed coexisting band built on the first excited 0^+ state. This assignment was later refuted [16], and the postulated γ band re-established as being built on the 2_2^+ level.

This paper uses the β decay of ^{74}Br to populate nonyrast levels in ^{74}Se in order to extend the data on the low-lying states and then investigate their mixing. Odd-odd ^{74}Br has $J = 0$ and $J = 4$ β -decaying states so population of almost all the known low-lying levels can be achieved. The higher spin β -decaying state in ^{74}Br , ($J^\pi = 4^{(+)}$) is particularly useful; it has a very unusual structure, being highly prolate-deformed, with a quadrupole moment corresponding to an axial ellipsoid with $\beta_2 \sim 0.4$ and also being a two-quasiparticle $K = 4$ isomer [17,18]. As β decay is both shape and K selective, we have an interesting starting point to investigate the overlap with the deformed states in the ^{74}Se daughter.

II. EXPERIMENT

^{74}Br parent nuclei were produced using the $^{60}\text{Ni}(^{16}\text{O}, pn)$ reaction with a 15-pnA, 52-MeV ^{16}O beam provided by the ESTU tandem accelerator at the Wright Nuclear Structure Laboratory at Yale University. The target was an 10-mg/cm² ^{60}Ni foil. Only the first ~ 4 mg/cm² of target yielded a significant production cross section for ^{74}Br , whereas the latter half of the target served to stop all the recoiling product nuclei. Excited levels in ^{74}Se were populated following the ϵ/β^+ decay of the ^{74}Br nuclei. ^{74}Br has two β -decaying

states [19], the ground state with spin and parity $J^\pi = (0^-)$ and $T_{1/2} = 25.4$ min and an isomeric state with spin and parity $J^\pi = 4^{(+)}$ and $T_{1/2} = 46$ min. The experiment was performed with a beam-on/beam-off cycle of 1 h. The decays from the ground state and the isomer have been studied independently in Ref. [20] and Refs. [21,22], respectively. Since the two β -decaying states are of sufficiently different J^π values, a number of levels are fed only from either the ground state or the isomer. By comparing the feeding and γ intensities obtained in this work with the results given in Refs. [20–22], it was determined that the majority of the decays observed in the present experiment originated from the $4^{(+)}$ isomer. The fraction of the produced ^{74}Br in the (0^-) ground state was found to be 7(3)%. This is consistent with what one might expect given the heavy-ion production mechanism for ^{74}Br which favor population of the higher spin level.

In the beam-off cycle, γ rays were detected with eight Compton-suppressed segmented YRAST Ball Clover HPG detectors. Both γ -ray singles and γ - γ coincidence data were collected in event mode. The photopeak efficiency of the array was $\sim 2\%$ at 1.3 MeV and covered an energy range from ~ 55 to 5000 keV. Four hours of data were collected with a singles trigger and 12 h of data were collected with a doubles trigger, yielding 1.6×10^8 Clover singles events and 8.5×10^7 Clover-Clover coincidence pairs, respectively.

The projection of the γ - γ coincidence matrix is shown in Fig. 1(a), illustrating the high density of observed γ -ray transitions. The reaction was very clean and the majority of observed lines belong to the decay of ^{74}Br to ^{74}Se . Contaminants observed in the spectrum were the decays of ^{73m}Se and ^{71}As ; however, their contribution was small and prior knowledge of their decay schemes [23,24] allowed for positive identification of their associated γ rays in the γ - γ coincidence matrix. The quality of the coincidence data is illustrated in Fig. 1(b) with a gate on the 634-/635-keV transitions corresponding to the closely spaced, 634.7-keV, $2_1^+ \rightarrow 0_1^+$ transition and the 634.3-keV, $2_2^+ \rightarrow 2_1^+$ transition, which could not be resolved in the present setup.

The level scheme was constructed mainly from γ - γ coincidence measurements which were also used to deduce the γ -ray intensities. Intensities of γ rays which directly populate the ground state were taken from the singles data, except in cases where a strong feeding transition into a level could be used to determine the relative intensities of the depopulating transitions. In the present work, no evidence is found for three levels previously proposed in β decay, 12 new levels are identified, and the decay properties of several levels are significantly modified. The levels populated in ^{74}Se and their γ decay are summarized in Table I. Branching ratios from excited levels are compared with the current literature [19] values. Levels which were observed in a previous study [20] of the decay of the $J^\pi = (0^-)$ ground state but not in the decay from the $J^\pi = 4^{(+)}$ isomer [21,22] are indicated by an asterisk. Figure 2 gives a partial level scheme of ^{74}Se for states below 2600 keV.

Angular correlation measurements were also performed with the Clover detectors positioned at relative, first-quadrant angles of 0° , 45° , 60° , and 90° . Of the 28 total detector pairs, only three were positioned at 180° to each other (equivalent

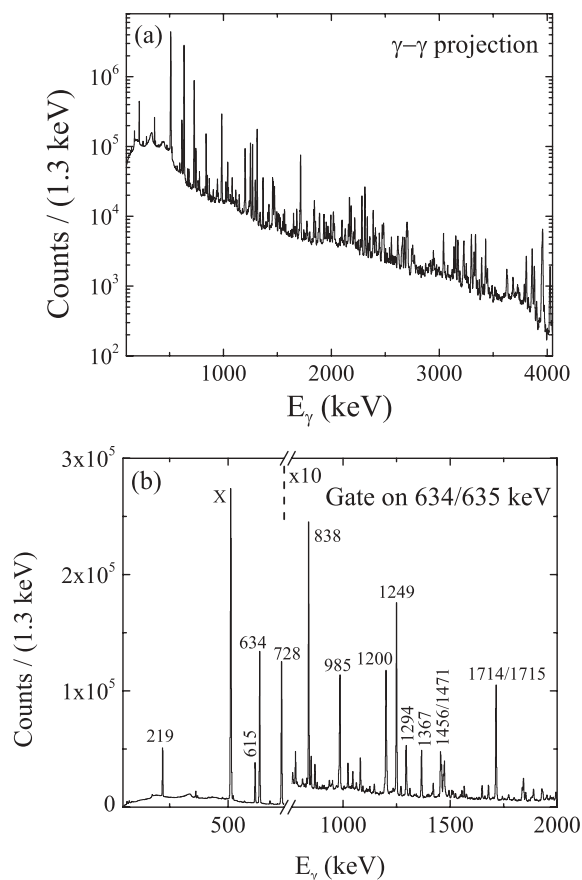


FIG. 1. (a) Projection of the γ - γ coincidence matrix. (b) Spectrum gated on the 634-/635-keV, $2_1^+ \rightarrow 0_1^+$ and $2_2^+ \rightarrow 2_1^+$ transitions in ^{74}Se . Intense transitions in ^{74}Se are labeled by their energy in keV. Note that in (b) the y scale is multiplied by a factor of 10 for $E_\gamma > 750$ keV. The peak labeled “x” arises from positron annihilation.

to 0° in the first quadrant angles). This limited the angular correlation analysis to strongly populated cascades. Results from the angular correlation measurement are given in Table II. The well-known 219–635 keV, $0_2^+ \rightarrow 2_1^+ \rightarrow 0_1^+$, and 728–635 keV, $4_1^+ \rightarrow 2_1^+ \rightarrow 0_1^+$ cascades, included in Table II, were used to confirm the measurement and analysis procedure. The A_2 and A_4 coefficients obtained for these cascades agree very well with what is expected from angular correlation theory. The $E2/M1$ mixing ratios given in Table II are in the sign convention of Krane and Steffen [25].

A. Discussion of levels

The level at 1269-keV decays by 634.3- and 1269-keV transitions to the 2_1^+ and 0_1^+ states, respectively. These transitions were observed and their intensities found to be consistent with the literature values. A new depopulating transition of 415.2 keV was identified corresponding to a decay to the 0_2^+ state. Evidence for this transition is given in Fig. 3. The 415-keV transition is observed in a gate on the 219-keV, $0_2^+ \rightarrow 2_1^+$ transition, as shown in Fig. 3(a). The peak is located quite close to the Compton edge of the very intense 634/635 doublet transition (corresponding to the bump in the

TABLE I. Levels populated in ^{74}Se following the ϵ/β^+ decay of ^{74}Br and their γ decay. Relative intensities for γ -ray transitions depopulating the levels are given. I_γ gives the intensity in β decay normalized to $2_1^+ \rightarrow 0_1^+ \equiv 100$, while B_γ gives the relative intensity from each level, normalized to the strongest branch. Relative intensities from each of the levels are also compared with literature values, B_{lit} [19], where available. Levels populated in the decay of the (0^-) ground state of ^{74}Br are indicated by an asterisk.

$J_i^{\pi^a}$	E_i (keV)	0^- decay	J_f^π	E_f (keV)	E_γ (keV)	I_γ	B_γ	B_{lit}^b
2^+	634.75(9)		0^+	0.00	634.75(9)	100(4)	100(4)	100
0^+	853.92(11)		2^+	634.75	219.17(7)	7.2(3)	100(4)	100(4)
2^+	1269.07(8)		0^+	0.00	1269.03(12)	9.7(5)	52(3)	52(3)
			2^+	634.75	634.31(12)	18.6(9)	100(5)	100(8)
			0^+	853.92	415.21(7) ^c	0.16(2)	0.86(11)	
4^+	1363.08(11)		2^+	634.75	728.33(8)	38.9(16)	100(4)	100
0^{+d}	1657.50(12)	*	2^+	634.75	1022.76(9)	0.87(7)	100(8)	100
			2^+	1269.07	388.2(3) ^c	0.06(2)	6.9(23)	
2^{+d}	1838.81(13)		2^+	634.75	1204.07(15)	1.2(2)	30(5)	22(11)
			0^+	853.92	984.88(9)	4.0(3)	100(8)	100(5)
			2^+	1269.07	569.84(15) ^c	0.20(4)	5(1)	
3^{+d}	1884.26(13)		2^+	634.75	1249.52(8)	7.7(4)	100(5)	89(12)
			2^+	1269.07	615.19(8)	7.4(4)	96(5)	100(8)
			4^+	1363.08	521.04(15)	0.9(1)	12(1)	10(3)
4^+	2107.97(15)		2^+	634.75	1473.31(11)	1.85(15)	28(2)	25(3)
			2^+	1269.07	838.93(8)	6.5(4)	100(6)	100(8)
			4^+	1363.08	744.77(15)	2.36(18)	36(3)	40(4)
6^+	2231.30(15)		4^+	1363.08	868.19(12)	0.73(5)	100(7)	100
2^{+d}	2313.97(11)		0^+	0.00	2314.15(23) ^c	0.15(4)	9.9(26)	
			2^+	634.75	1679.20(12)	0.66(5)	44(3)	92(10)
			0^+	853.92	1460.13(11)	1.51(9)	100(6)	100(8)
			2^+	1269.07	1044.90(12)	0.52(3)	34(2)	46(5)
			4^+	1363.08	950.8(2) ^c	0.24(3)	15.9(20)	
			0^+	1657.50	656.50(20) ^c	0.055(13)	3.6(9)	
			2^+	1838.81	475.16(12) ^c	0.29(3)	19.2(20)	
			3^+	1884.26	429.74(13) ^c	0.11(3)	7.3(20)	
3^-	2349.83(20)		2^+	634.75	1715.20(13)	1.06(10)	100(10)	91(9)
			2^+	1269.07	1080.65(20)	0.88(7)	83(7)	100(14)
			4^+	1363.08	986.7(2)	0.83(8)	78(8)	57(11)
$(1,2^+)$	2379.1(3)	*	2^+	634.75	1744.6(2)	0.19(2)	100(11)	100(28)
			0^+	853.92	1524.9(2)	0.039(5)	21(3)	28(6)
			2^+	1269.07	1110.0(3)	0.12(3)	63(16)	50(6)
(2^+)	2488.25(18) ^c		0^+	0.00	2488.32(18) ^c	0.49(5)	98(10)	
			2^+	634.75	1853.48(17) ^c	0.50(4)	100(8)	
			0^+	853.92	1634.5(2) ^c	0.14(2)	28(4)	
			0^+	1657.50	830.6(2) ^c	0.22(3)	44(6)	
			2^+	1838.81	649.4(2) ^c	0.11(3)	22(6)	
$(2^+,3,4^+)$	2563.38(15)		2^+	634.75	1928.8(3)	0.71(5)	14(1)	12(2)
			2^+	1269.07	1294.40(11)	1.75(15)	35(3)	39(5)
			4^+	1363.08	1200.25(10)	5.0(3)	100(6)	100(11)
			2^+	1838.81	724.5(3)	0.69(5)	14(1)	12(5)
			3^+	1884.26	679.09(12)	0.82(5)	16(1)	12(2)
5^+	2661.79(15)		2^+	634.75	[2028] ^f	<0.04	<5	
			4^+	1363.08	1298.7(2)	0.37(4)	51(5)	47(16)
			3^+	1884.26	777.50(13)	0.73(4)	100(5)	100(7)
			4^+	2107.97	553.9(3) ^c	0.085(20)	11.6(27)	
$(2^+,3,4^+)$	2818.51(13)		2^+	634.75	2183(1) ^{c,g}	0.55(6)	26(3)	
			4^+	1363.08	1455.38(11)	2.12(15)	100(7)	100(15)
			2^+	1838.81	979.74(15)	0.48(4)	23(2)	25(5)
			3^+	1884.26	934.36(20) ^c	0.16(2)	7.5(9)	
4^-	2831.49(13)		4^+	1363.08	1468.37(11)	1.09(8)	100(7)	100(13)
			3^+	1884.26	947.2(3) ^c	0.080(8)	7.3(7)	

TABLE I. (*Continued.*)

$J_i^{\pi a}$	E_i (keV)	0^- decay	J_f^{π}	E_f (keV)	E_γ (keV)	I_γ	B_γ	B_{lit}^b
$(2^+, 3, 4^+)$	2918.32(16)		2^+	634.75	2283.61(12)	3.1(2)	100(6)	100(15)
			2^+	1269.07	1649.21(15)	0.54(4)	17(1)	14(2)
			4^+	1363.08	1555.26(15)	0.41(4)	13(1)	13(2)
			2^+	1838.81	1079.7(3)	0.30(3)	9.7(10)	19(4)
4^{+h}	3077.59(20)		4^+	2107.97	810.36(18) ^c	0.20(2)	6.5(6)	
			2^+	634.75	[2443] ^f	<0.04	<0.8	6.0(15)
			4^+	1363.08	1714.7(2)	5.1(3)	100(6)	100(10)
			3^+	1884.26	1193.29(18)	0.29(2)	5.7(4)	1.5(3)
			6^+	2231.30	846.3(3) ^e	0.024(9)	0.5(2)	
			2^+	2313.97	763.66(18)	0.28(3)	5.5(6)	3.7(8)
(4)	3200.11(15)		4^+	1363.08	1837.14(13)	0.69(4)	79(5)	50(15)
			4^+	2017.97	1092.04(18) ^c	0.19(2)	22(2)	
			3^-	2349.83	850.25(15) ^h	0.87(4)	100(5)	100(50)
			4^-	2831.49	368.64(9) ^h	0.36(2)	41(2)	50(10)
$(1, 2^+)$	3250.3(3)		0^+	0.00	3250.5(4)	0.85(9)	79(8)	83(4)
			2^+	634.75	2615.7(3)	1.07(8)	100(8)	100(3)
			0^+	853.92	2397.4(3)	0.245(16)	23(2)	38(2)
			2^+	1269.07	1982.0(3)	0.27(3)	25(3)	18(1)
			2^+	2313.97	937.9(3) ^g	0.11(2)	10(2)	10(2)
			$(1, 2^+)$	2379.1	871.6(3) ^g	0.05(3)	5(3)	3.5(17)
			3^+	1884.26	1366.64(15)	2.12(18)	100(8)	100
			4^+	1368.08	1890.21(15)	0.73(5)	100(7)	100
			2^+	1838.81	1414.45(20) ^c	0.18(4)	25(5)	
			4^+	2107.97	1145.41(18) ^c	0.29(3)	40(4)	
$(2^+, 3, 4^+)^h$	3250.9(2)		3^-	2349.83	903.5(2) ^e	0.13(1)	18(2)	
	3253.3(2)		$(2^+, 3, 4^+)$	2563.38	689.8(2) ^e	0.20(5)	27(7)	
			3^+	1884.26	1421.10(12)	0.53(3)	100(6)	100(14)
			4^+	2107.97	1197.30(15)	0.27(3)	51(6)	57(14)
			$(2^+, 3, 4^+)$	2563.38	741.8(4) ^e	0.38(2)	72(4)	
$(3^+, 4, 5^+)^h$	3305.32(18)		5^+	2661.79	643.5(5) ^e	0.088(21)	17(4)	
			2^+	634.75	2745.0(4)	0.33(4)	100(12)	91(23)
			4^+	1368.08	2016.3(3) ^e	0.23(5)	70(15)	
			2^+	1838.81	1540.8(2) ^e	0.073(12)	22(4)	
(2^+)	3379.5(2)		3^+	1884.26	1495.20(15)	0.28(2)	85(6)	100(14)
			4^+	2107.97	1271.2(4) ^e	0.16(4)	48(12)	
			0^+	0.00	3541.1(3)	0.060(7)	26(3)	38(8)
			2^+	634.75	[2904] ^f	<0.14	<60	100(8)
			0^+	853.92	2686.2(3)	0.017(7)	7.4(30)	15(8)
			2^+	1269.07	2271.1(4)	0.23(4)	100(17)	100(19)
$(1, 2^+)$	3540.0(2)	*	0^+	1657.50	1882.56(18)	0.112(15)	49(7)	96(12)
			2^+	1838.81	1701.0(3)	0.086(18)	38(8)	46(8)
			2^+	2313.97	1225.8(5)	0.13(2)	57(13)	81(8)
			2^+	634.75	[2945] ^f	<0.04	<5	<60
			4^+	1368.08	2216.89(15)	0.69(5)	100(7)	100(20)
			0^+	0.00	3625.6(4)	0.60(3)	100(5)	100(5)
(2^+)	3579.97(18)		0^+	853.92	2771.24(18)	0.15(1)	25(2)	37(2)
			2^+	634.75	3039.7(3)	0.65(6)	23(2)	<32
			4^+	1368.08	2310.99(15)	2.84(21)	100(7)	100(14)
$(2^+, 3, 4^+)$	3674.05(13)		4^+	2107.97	1566.06(15)	0.53(3)	19(1)	10(2)
			2^+	1269.07	2413.8(4) ^e	0.26(4)	100(15)	
			3^+	1884.26	1799.0(4) ^e	0.095(15)	37(6)	
			4^+	2107.97	1574.9(2) ^e	0.11(2)	42(8)	
			2^+	634.75	3137.25(16)	0.63(5)	100(8)	70(10)
(4^+)	3771.97(15)		2^+	1269.07	2503.2(3)	0.20(3)	32(5)	19(5)
			4^+	1368.08	2408.84(18)	0.34(3)	54(5)	100(40)
			2^+	1838.81	1933.12(16)	0.40(4)	63(6)	50(10)
			3^+	1884.26	1887.78(18) ^c	0.16(3)	25(5)	

TABLE I. (Continued.)

$J_i^{\pi a}$	E_i (keV)	0^- decay	J_f^{π}	E_f (keV)	E_{γ} (keV)	I_{γ}	B_{γ}	B_{lit}^b
(1,2 ⁺)	3788.5(2)	*	0 ⁺	0.00	3788.7(3)	0.37(4)	100(11)	100(5)
			0 ⁺	853.92	2934.8(4)	0.039(8)	11(2)	19(3)
			0 ⁺	1657.50	2130.94(13)	0.254(20)	69(5)	71(3)
			2 ⁺	1838.81	1949.6(3)	0.16(2)	43(5)	37(3)
			2 ⁺	2313.97	1474.6(3)	0.12(3)	32(8)	27(3)
			2 ⁺	1269.07	2539.5(4) ^c	0.22(5)	59(13)	
			4 ⁺	1368.08	2445.13(18) ^c	0.375(24)	100(7)	
			4 ⁺	1368.08	2451.0(2) ^c	0.13(2)	33(5)	
			3 ⁺	1884.26	1930.0(5) ^c	0.11(3)	28(8)	
			(2 ⁺ ,3,4 ⁺)	2563.38	1250.64(15) ^c	0.40(4)	100(10)	
(0 ⁺ ,1)	3931.95(25)	*	2 ⁺	634.75	3297.0(5)	0.40(6)	74(11)	53(3)
			2 ⁺	1269.07	2662.9(3)	0.54(3)	100(6)	100(6)
			2 ⁺	1269.07	2681.5(3) ^c	0.23(5)	100(22)	
			4 ⁺	2107.97	1842.30(23) ^c	0.10(2)	44(9)	
(2 ⁺)	3973.4(3)	*	0 ⁺	0.00	3973.2(5)	0.19(2)	100(11)	100(6)
			2 ⁺	634.75	(3339)	_i		19(6)
			0 ⁺	853.92	3119.5(3)	0.067(7)	35(4)	39(6)
			2 ⁺	1269.07	(2704)	_i		67(6)
			2 ⁺	1269.07	2768.4(3) ^c	0.16(5)	100(31)	
			4 ⁺	1363.08	2674.3(5) ^c	0.13(2)	81(13)	
			4 ⁺	1368.08	2679.2(2) ^c	0.235(25)	100(11)	
(1,2 ⁺)	4045.0(3)	*	4 ⁺	2107.97	1934.3(3) ^c	0.096(15)	41(7)	
			0 ⁺	0.00	4044.8(4)	0.11(2)	100(18)	87(13)
			2 ⁺	634.75	[3410] ^f	<0.031	<28	40(13)
			0 ⁺	853.92	3191.04(15)	0.095(8)	86(7)	100(13)
			0 ⁺	1657.50	[2387]	<0.03	<28	47(13)
(2 ⁺)	4095.1(2)	*	0 ⁺	0.00	4095.0(3)	0.040(6)	71(11)	38(10)
			2 ⁺	634.75	[3460] ^f	<0.05	<89	90(10)
			0 ⁺	853.92	3241.17(25)	0.056(9)	100(16)	48(10)
			0 ⁺	1657.50	2437.7(3)	0.036(9)	64(16)	52(10)
			(1,2 ⁺)	2379.1	0.029(5)	52(9)	100(14)	
(1,2 ⁺)	4266.6(3)	*	0 ⁺	0.00	4266.4(3)	0.12(2)	69(12)	43(8)
			2 ⁺	634.75	3631.8(4)	0.175(15)	100(9)	100(8)
			4 ⁺	1368.08	2919.5(4) ^{c,g}	0.077(13)	29(5)	
			2 ⁺	1838.81	2443.8(2) ^c	0.089(20)	33(8)	
			3 ⁺	1884.26	2397.9(2) ^c	0.12(2)	45(8)	
			2 ⁺	2313.97	1968.17(18) ^c	0.27(4)	100(15)	
(3,4 ⁺)	4309.15(16)	*	2 ⁺	1269.07	3040.2(2)	0.82(6)	100(7)	<240
			4 ⁺	1368.08	2946.09(18)	0.33(3)	40(4)	<60
			4 ⁺	2107.97	2201.2(3) ^c	0.088(23)	10.7(28)	
			2 ⁺	2313.97	1995.10(15)	0.57(5)	70(6)	100(20)
			3 ⁻	2349.83	1959.0(3) ^c	0.055(13)	6.7(16)	
			(2 ⁺ ,3,4 ⁺)	2563.38	[1746] ^f	<0.04	<5	28(10)
			4 ⁻	2831.49	1477.73(20) ^c	0.099(22)	12(2)	
			2 ⁺	1269.07	3049.2(4) ^c	0.27(6)	100(22)	
			4 ⁺	1368.08	2955.4(5) ^c	0.10(2)	37(8)	
			4 ⁺	2107.97	2210.64(25) ^c	0.12(2)	45(8)	
(2 ⁺)	4343.3(3)	*	2 ⁺	2313.97	2004.7(4) ^c	0.10(3)	37(11)	
			(2 ⁺ ,3,4 ⁺)	2918.32	1400.0(4) ^c	0.098(17)	36(6)	
			0 ⁺	0.00	4343.0(5)	0.12(2)	100(17)	100(14)
			0 ⁺	853.92	3489.4(3)	0.037(5)	31(4)	29(10)
			4 ⁺	2107.97	2252.8(4) ^{c,g}	0.16(3)	100(19)	
			4 ⁻	2831.49	1528.9(2) ^c	0.065(14)	41(9)	
			0 ⁺	0.00	4380.4(5)	0.36(2)	100(6)	100(6)
(1,2 ⁺)	4380.6(3)	*	2 ⁺	634.75	3746.3(7)	0.055(17)	15(5)	15(3)
			0 ⁺	853.92	3526.64(19)	0.057(6)	16(2)	15(3)

TABLE I. (*Continued.*)

$J_i^{\pi a}$	E_i (keV)	0^- decay	J_f^{π}	E_f (keV)	E_γ (keV)	I_γ	B_γ	B_{lit}^b			
(3,4 ⁺)	4441.41(13)		2 ⁺	634.75	3806.8(3)	0.90(8)	95(8)	100(17)			
			2 ⁺	1269.07	3172.5(2)	0.55(5)	58(5)	100(17)			
			4 ⁺	1368.08	3078.3(2) ^c	0.13(2)	14(2)				
			3 ⁺	1884.26	2557.20(15) ^c	0.43(3)	45(3)				
			4 ⁺	2107.97	2333.28(15)	0.95(6)	100(6)	75(8)			
			(2 ⁺)	2488.25	1953.24(20) ^c	0.34(3)	36(3)				
			(2 ⁺ ,3,4 ⁺)	2563.38	1877.88(23) ^c	0.12(2)	12.6(21)				
			(2 ⁺ ,3,4 ⁺)	2918.32	1522.5(4) ^c	0.029(8)	3.1(9)				
			(2 ⁺)	3379.5	1061.7(2) ^c	0.30(4)	32(4)				
			(3,4 ⁺)	4496.12(13)		2 ⁺	634.75	3861.4(2)	1.25(10)	100(8)	100(19)
2 ⁺	1269.07	3227.09(22)				0.42(4)	34(3)	<56			
2 ⁺	1838.81	2657.24(19) ^c				0.22(2)	18(2)				
3 ⁺	1884.26	2611.9(3) ^c				0.12(3)	9.6(24)				
4 ⁺	2107.97	2388.11(15)				1.06(8)	85(6)	81(13)			
2 ⁺	2313.97	2182.22(15) ^c				0.87(7)	70(6)				
4 ⁻	2831.49	1664.7(3) ^c				0.026(9)	2.1(7)				
(2 ⁺ ,3,4 ⁺)	2918.32	1577.6(3) ^c				0.14(4)	11.2(16)				
3 ⁺	1884.26	2622.5(3) ^{c,e}				0.084(21)	98(25)				
(2 ⁺ ,3,4 ⁺)	2563.38	1943.1(2) ^c				0.086(20)	100(23)				
(3,4 ⁺)	4506.5(3) ^e		2 ⁺	634.75	3881.6(3)	0.67(6)	79(7)	83(9)			
			2 ⁺	1269.07	[3247] ^f	<0.03	<4	<45			
			4 ⁺	1368.08	3152.97(14)	0.85(5)	100(6)	100(18)			
			2 ⁺	1838.81	2677.25(20) ^c	0.12(4)	14(5)				
			4 ⁺	2107.97	2408.38(20) ^c	0.16(2)	19(2)				
			(2 ⁺)	2488.25	2027.7(2) ^c	0.12(3)	14(4)				
			(2 ⁺ ,3,4 ⁺)	2563.38	[1952] ^f	<0.03	<4	32(6)			
			5 ⁺	2661.79	[1854] ^f	<0.01	<1	45(9)			
			(1,2 ⁺)	4537.0(4)	*	0 ⁺	0.00	4537.3(5)	0.016(2)	11(2)	9(5)
						2 ⁺	634.75	3902.5(3)	0.15(2)	100(13)	100(9)
2 ⁺	1269.07	3267.6(4)				0.096(16)	64(11)	36(9)			
(3,4,5)	4579.9(2)		3 ⁺	1884.26	2695.73(26)	0.68(4)	100(6)	100(13)			
			4 ⁺	2107.97	2471.86(20)	0.59(3)	87(4)	100(13)			
(3,4 ⁺)	4585.85(12)		2 ⁺	634.75	3951.0(4)	1.05(15)	100(14)	92(15)			
			2 ⁺	1838.81	2747.0(3) ^c	0.16(3)	15(3)				
			3 ⁺	1884.26	2701.6(2)	1.01(9)	96(9)	100(15)			
			4 ⁺	2107.97	2477.9(2)	0.45(3)	43(3)	<38			
			(2 ⁺)	2488.25	2097.4(3) ^c	0.082(9)	7.8(9)				
			(2 ⁺ ,3,4 ⁺)	2563.38	2022.55(20) ^c	0.16(3)	15(3)				
			4 ⁻	2831.49	1754.36(25) ^c	0.058(12)	5.5(11)				
(4 ⁺)	4592.45(25)		4 ⁺	3077.59	1508.12(23)	0.37(4)	35(4)	18(4)			
			2 ⁺	634.75	3957.9(4)	2.7(2)	100(7)	100(12)			
			2 ⁺	1269.07	3323.6(3)	0.62(5)	23(2)	15(3)			
			4 ⁺	1368.08	3229.2(3)	0.45(5)	17(2)	<22			
			2 ⁺	1838.81	2753.9(3) ^c	0.30(3)	11(1)				
			3 ⁺	1884.26	2708.06(20)	0.71(5)	26(2)	15(3)			
			4 ⁺	2107.97	2484.65(15)	0.72(5)	27(2)	10(3)			
			(2 ⁺)	2488.25	2104.0(4) ^c	0.032(4)	1.2(2)				
			(2 ⁺ ,3,4 ⁺)	2563.38	2029.07(18)	0.25(3)	9(1)	<12			
			4 ⁺	3077.59	1515.0(4) ^c	0.10(3)	3.7(11)				
(3,4 ⁺)	4623.5(3) ^e		4 ⁺	1368.08	3260.4(3) ^c	0.12(2)	100(17)				
			4 ⁺	2107.97	2515.7(2) ^c	0.12(2)	100(17)				
			2 ⁺	634.75	4027.1(4)	0.80(7)	90(8)	80(13)			
			2 ⁺	1269.07	3393.0(3)	0.42(3)	47(3)	<40			
(3,4 ⁺)	4661.84(23)		4 ⁺	1368.08	3298.59(17)	0.89(7)	100(8)	100(20)			
			2 ⁺	1838.81	[2825] ^f	<0.01	<1				
			(2 ⁺ ,3,4 ⁺)	2563.38	2098.48(15)	0.52(4)	58(4)	33(7)			

TABLE I. (Continued.)

$J_i^{\pi a}$	E_i (keV)	0^- decay	J_f^{π}	E_f (keV)	E_{γ} (keV)	I_{γ}	B_{γ}	B_{lit}^b
(3,4 ⁺)	4699.2(2)		2 ⁺	634.75	4064.7(4)	0.12(3)	11(3)	16(5)
			2 ⁺	1269.07	3430.2(2) ^c	0.30(6)	27(6)	
			4 ⁺	1368.08	3336.08(13)	1.11(10)	100(9)	100(15)
			4 ⁺	2107.97	2591.0(3) ^c	0.14(2)	12.6(18)	
(3,4 ⁺)	4758.1(2)		2 ⁺	634.75	4126.0(5)	0.076(8)	42(5)	120(8)
			4 ⁺	1368.08	3395.7(4)	0.13(3)	72(17)	<100
			3 ⁺	1884.26	2874.0(3) ^c	0.14(3)	78(17)	
			4 ⁺	2107.97	2650.06(15) ^c	0.18(3)	100(17)	
			(4 ⁺)	3771.97	[1022] ^f	<0.02	<3	31(4)

^aLevel spin assignments are nominal assignments from the evaluation [19], except as noted.

^bLiterature values for branches are from the evaluated data [19].

^cNewly observed γ -ray transition.

^dSpin assignment for previously observed level determined from angular correlation measurements in the present work.

^eNewly observed level.

^fPreviously reported transition, coincidence data from present work finds no evidence for the transition.

^gTentative placement.

^hNew spin assignment for previously observed level is given on the basis of observed transitions to levels of known spin.

ⁱPreviously observed transition, placement could not be verified in the present work due to overlapping transitions of similar energy which could not be resolved.

energy spectrum at ~ 450 keV), which could be the reason prior studies had failed to identify the transition. A gate on the 415-keV transition, Fig. 3(b), reveals the depopulating cascade of the 219- and 635-keV transitions, as well as the two strong transitions (615 and 839 keV) which populate the 1269-keV level. The observation of the new γ -ray branch combined with the measured lifetime of $T_{1/2} = 75(5)$ ns [19]

gives a $B(E2)$ value of 3.5(11) W.u. for the $0_2^+ \rightarrow 2_1^+$ transition.

Angular correlation analysis of the 634- to 635-keV cascade yielded a δ value of ≤ -30 for the $2_2^+ \rightarrow 2_1^+$ transition. Reference [21] reported $|\delta| > 50$, also from $\gamma\gamma(\theta)$ measurements. The evaluated data [19] reports a value of $\delta = -5.6(16)$ based on the A_2 and A_4 values given in Ref. [21]. The results from the

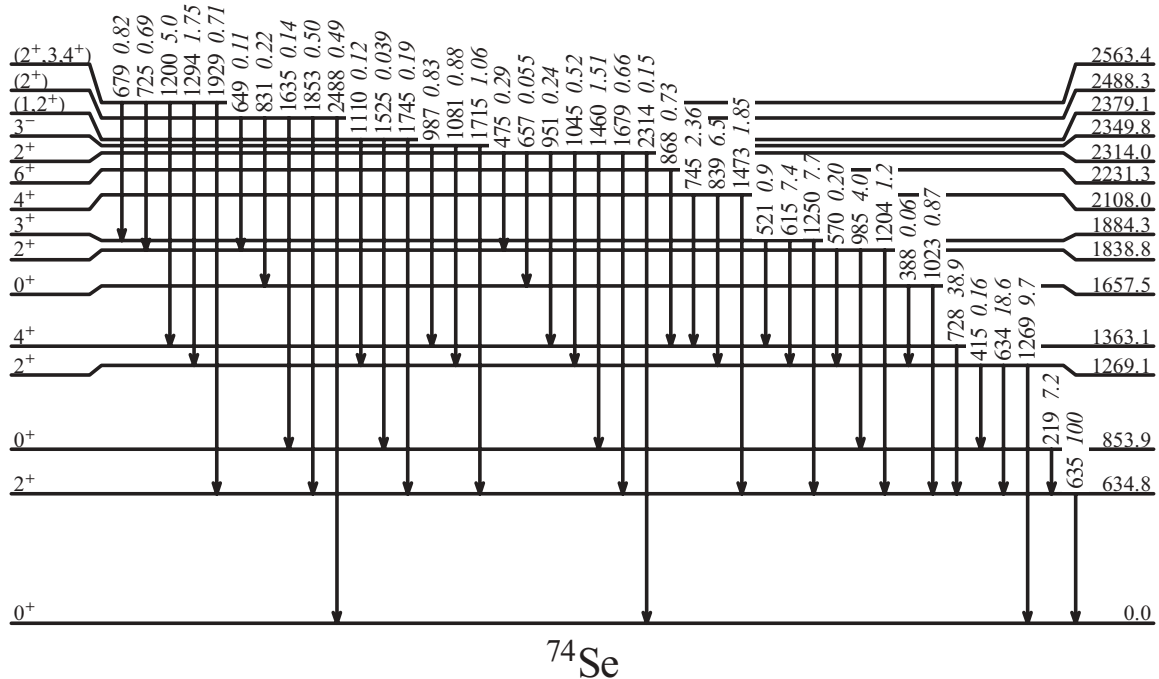


FIG. 2. Partial level scheme of ^{74}Se populated in the ϵ/β^+ decay of ^{74}Br . Levels and transitions are labeled by their energy in keV. The relative intensity of the γ -ray transitions is included in italics, normalized to the 635-keV, $2_1^+ \rightarrow 0_1^+$ transition ($I_{635} \equiv 100$). Additional levels in the energy range 2600–4800 keV are summarized in Table I.

TABLE II. Results of the angular correlation measurement. The first two columns give the pair of γ transitions considered in the analysis and their corresponding spin sequence. The A_2 and A_4 coefficients are obtained from fits of the angular correlation data to the sum of Legendre Polynomials $1 + A_2 P_2(\cos\theta) + A_4 P_4(\cos\theta)$. The δ values are derived from the fits and given in the convention of Krane and Steffen [25].

Cascade (keV)	Spin sequence	A_2	A_4	Mult	δ
219–635	$0_2^+ \rightarrow 2_1^+ \rightarrow 0_1^+$	+0.31(5)	+0.95(6)	$E2$	
728–635	$4_1^+ \rightarrow 2_1^+ \rightarrow 0_1^+$	+0.102(3)	−0.007(5)	$E2$	
634–635	$2_2^+ \rightarrow 2_1^+ \rightarrow 0_1^+$	−0.049(3)	+0.218(7)	$E2(+M1)$	≤ -30
1022–635	$0_3^+ \rightarrow 2_1^+ \rightarrow 0_1^+$	+0.30(13)	+1.01(16)	$E2$	
1204–635	$2_3^+ \rightarrow 2_1^+ \rightarrow 0_1^+$	+0.16(8)	−0.015(7)	$M1+E2$	+0.09(8)
1250–635	$3_1^+ \rightarrow 2_1^+ \rightarrow 0_1^+$	+0.085(21)	−0.070(19)	$E2(+M1)$	+2.4(3)
615–1269	$3_1^+ \rightarrow 2_2^+ \rightarrow 0_1^+$	−0.0879(16)	−0.0323(15)	$M1$ or $E2$	−0.03(7) or +7(2)
521–728	$3_1^+ \rightarrow 4_1^+ \rightarrow 2_1^+$	−0.33(3)	−0.115(20)	$E2(+M1)$	+2.0(7)
745–728	$4_2^+ \rightarrow 4_1^+ \rightarrow 2_1^+$	−0.120(7)	+0.149(6)	$E2(+M1)$	>5
1679–635	$2_4^+ \rightarrow 2_1^+ \rightarrow 0_1^+$	−0.27(4)	+0.17(5)	$M1+E2$	+1.1(5)
1045–1269	$2_4^+ \rightarrow 2_2^+ \rightarrow 0_1^+$	+0.16(8)	−0.015(7)	$M1+E2$	−2.2 $^{+0.5}_{-0.9}$

present analysis and those of Refs. [19,21] are all consistent with nearly pure $E2$ character for the 634.3-keV, $2_2^+ \rightarrow 2_1^+$ transition.

A level at 1657.5 keV was proposed to decay via a single 1023-keV depopulating transition to the 2_1^+ state and tentatively assigned a J^π value of (0^+) by Ref. [19] based on the nonobservation of decays to 4^+ and 0^+ levels. As shown in Fig. 4(a), angular correlation analysis of the 1023-keV transition confirms the 0^+ spin assignment to this level. Included for comparison in Fig. 4(a) is the angular correlation analysis of the 219-keV transition from the well-established 0_2^+ state. Both correlations show a pronounced variation in $W(\theta)$ characteristic of a 0-2-0 cascade. An additional depopulating transition of 388.2 keV is observed in the present work as a transition to the 2_2^+ state.

The level at 1838 keV was reported [19] to decay by two depopulating transitions to the 2_1^+ and 0_2^+ levels and tentatively assigned a J^π value of (2^+) . In the present work, a new transition of 570 keV to the 2_2^+ is observed with a relative intensity of 5(1) compared with the strong 985-keV transition to the 0_2^+ level ($I = 100$). Angular correlation analysis confirms the 2^+ spin assignment of this level. The δ value for the 1204-keV, $2_3^+ \rightarrow 2_1^+$ transition was previously measured [26] in nuclear orientation as +0.18(7) or +1.5(2). In the present work, the best fit of the angular correlation for the 1204- to 635-keV cascade is found with $\delta = +0.09(8)$, as shown in Fig. 4(b). This result favors the smaller of the possible δ values proposed in Ref. [26] and nearly pure $M1$ character for the 1204 keV, $2_3^+ \rightarrow 2_1^+$ transition. For comparison, the solution with $\delta = +1.5$ is included in Fig. 4(b), which is not consistent with the current data.

A level at 1884 keV is reported [19] based on three depopulating transitions to the 4_1^+ , 2_2^+ , and 2_1^+ levels. These transitions are confirmed in the present work and found to have intensities consistent with those in the literature. There has been some controversy over the spin assignment of the 1884-keV level, with $J^\pi = 3^+$ or 4^+ postulated. A summary of the past measurements and proposed spin assignments is given in Ref. [16]. In the present work, the angular correlation analysis of all three depopulating transitions confirms the

3^+ spin assignment. For the 1250-keV, $3_1^+ \rightarrow 2_1^+$ transition, the δ value is determined for the first time as +2.4(3). The quality of the fit is shown in Fig. 5(a). In the analysis of the 521-keV, $3_1^+ \rightarrow 4_1^+$ transition, $\delta = +2.0(7)$ was obtained, as also illustrated in Fig. 5(a). In-beam $\gamma\gamma(\theta)$ measurements [11] determined $\delta = +0.3(1)$ for the 615-keV, $3_1^+ \rightarrow 2_2^+$ transition. In the present work, an equally good description of the angular correlation data could be obtained with $\delta = -0.03(7)$ or $\delta = +7(2)$, as shown in Fig. 5(b).

The level at 2108 keV is based on three depopulating transitions and assigned a spin of 4^+ based on $\gamma(\theta)$, $\gamma\gamma(\theta)$ measurements and band assignments from in-beam studies [19]. Reference [21] suggested that the 2108-keV level is in fact a closely spaced doublet based on their observation that the 2388-keV γ ray populating the 2108-keV level was observed in coincidence with the 839-keV depopulating transition but not the 745-keV depopulating transition. The present work finds no evidence for the proposed closely spaced doublet of levels, with support given in Fig. 6. In a gate on the 2388-keV γ ray, all three depopulating transitions of 745-, 839-, and 1473 keV are clearly observed along with the decays from low-lying levels which they populate. The mixing ratio of the 745-keV, $4_2^+ \rightarrow 4_1^+$ transition was determined to be $\delta = -4.3(3)$ or 2.4(2) in a nuclear orientation study [26]. In the present work, the angular correlation analysis finds $|\delta| > 5$, indicating nearly pure $E2$ character for the 745-keV transition.

The level at 2314 was previously proposed on the basis of three depopulating transitions to the 2_1^+ , 0_2^+ , and 2_2^+ levels. These transitions were observed with some modification to the literature intensities (see Table I). Four additional depopulating transitions were determined from the present γ - γ coincidence data. Support for these transitions is given in Fig. 7, using a gate on the 1995-keV transition which populates the 2314 level. While the 1995-keV transition is rather weak, nevertheless, all seven depopulating transitions are clearly observed in this spectrum. The newly observed transition to the 4_1^+ state, combined with two transitions to 0^+ states, suggests a spin-parity assignment of 2^+ based on the decay properties. This is confirmed by the angular correlation analysis of the 1679-keV transition as given in Fig. 4(c).

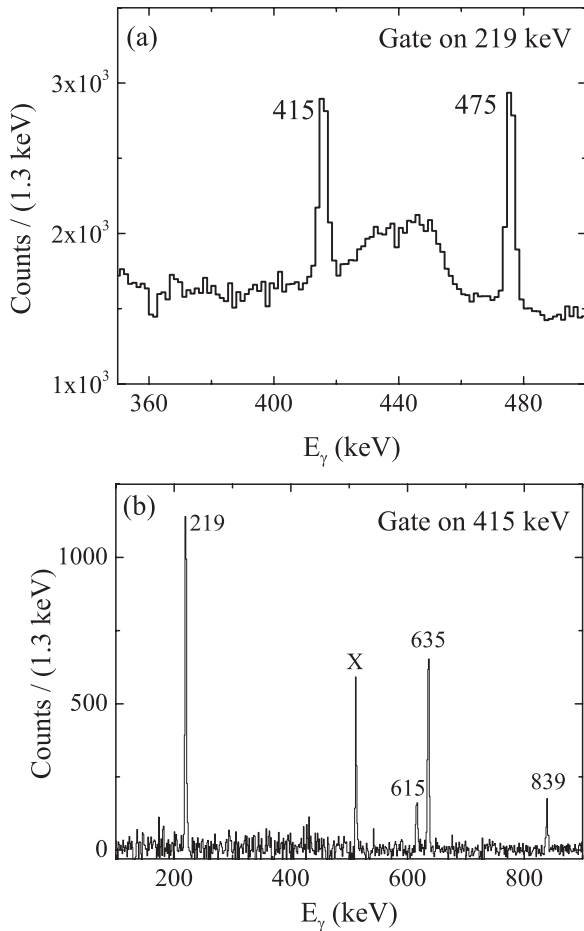


FIG. 3. Support for a 415-keV, $2_2^+ \rightarrow 0_2^+$ transition newly identified in the present work. (a) Spectrum gated on the 219-keV, $0_2^+ \rightarrow 2_1^+$ transition. The bump around 450 keV corresponds to the Compton edge of the very strong 634-/635-keV doublet. (b) Spectrum gated on the 415-keV, $2_2^+ \rightarrow 0_2^+$ transition. Gamma rays in ^{74}Se are labeled by their energy in keV and the 511-keV annihilation line is labeled with an X.

A new level is observed at 2488.3 keV, supported by the observation of five depopulating transitions. Evidence for this new level is given in Fig. 8, using a gate on the 1953-keV transition which was found to populate the level. In Fig. 8, the five newly observed depopulating transitions can be seen; their placement also confirmed by gating on γ rays from the levels which they feed into. As the decay of this new level is only observed to 0^+ and 2^+ states, a spin assignment of $(1, 2^+)$ is suggested. Statistics were too low to perform angular correlation analysis on any of the depopulating transitions. A level at 2482(25) keV was previously observed in the (p, t) reaction [27] which could correspond to the newly observed 2488.3 level. The L transfer in (p, t) gives a tentative spin assignment of (2^+) to this level, which is adopted here.

The present measurements resulted in several additional changes to the previously known level scheme of ^{74}Se which are summarized in Table I. In this work, no support is found for the previously proposed levels [21] at 3037, 3112, and 3929 keV. Twelve additional new levels are reported, each supported by two or more depopulating transitions. For many

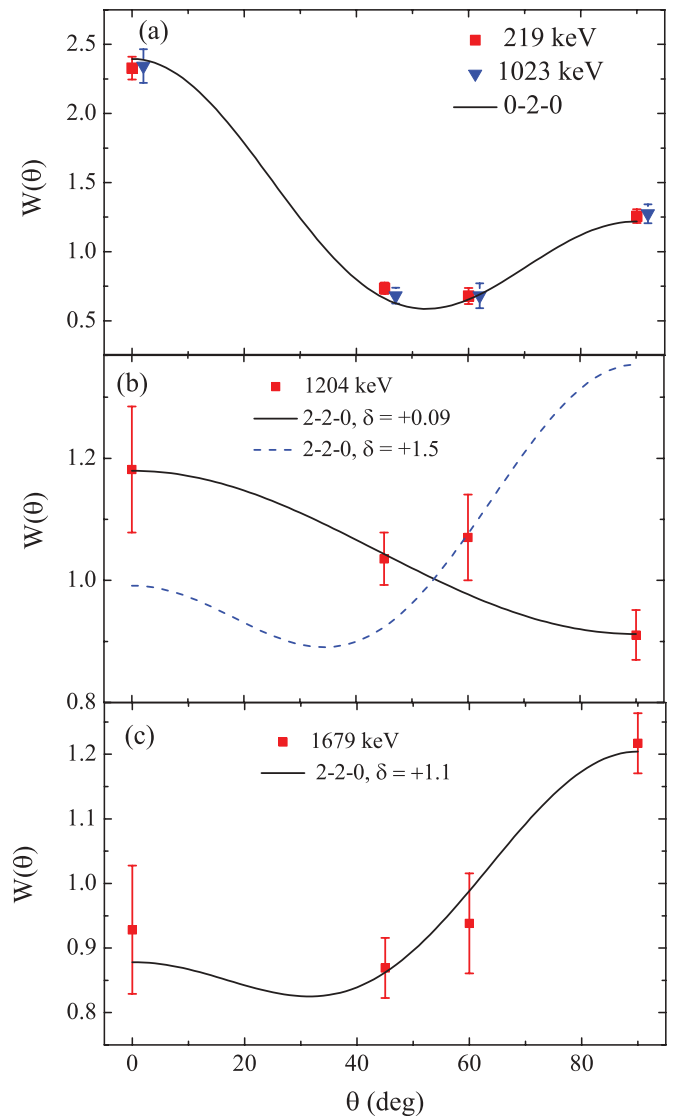


FIG. 4. (Color online) Angular correlation analysis for the (a) 219-keV and 1023-keV transitions, (b) the 1204-keV transition, and (c) the 1679-keV transition. Data are indicated by the symbols and compared with the theoretical prediction given by the lines. The theoretical curves are labeled by the assumed spin sequence and δ value.

of the previously reported levels, additional weak depopulating transitions are observed in the present high-statistics data.

III. DISCUSSION

A. Shape coexistence

Several prior works have proposed a shape-coexistence picture for ^{74}Se . At high-spin, a number of regular-rotational bands are observed [16], whereas for the low-spin states ($J \leq 6 \hbar$) this regularity is lost, providing evidence for mixing of shapes with different deformations. The original proposal [10] of the first excited 0^+ state being a deformed prolate intruder, which then develops into the yrast band at higher spin, can be tested by our present data. Such an interpretation was based on

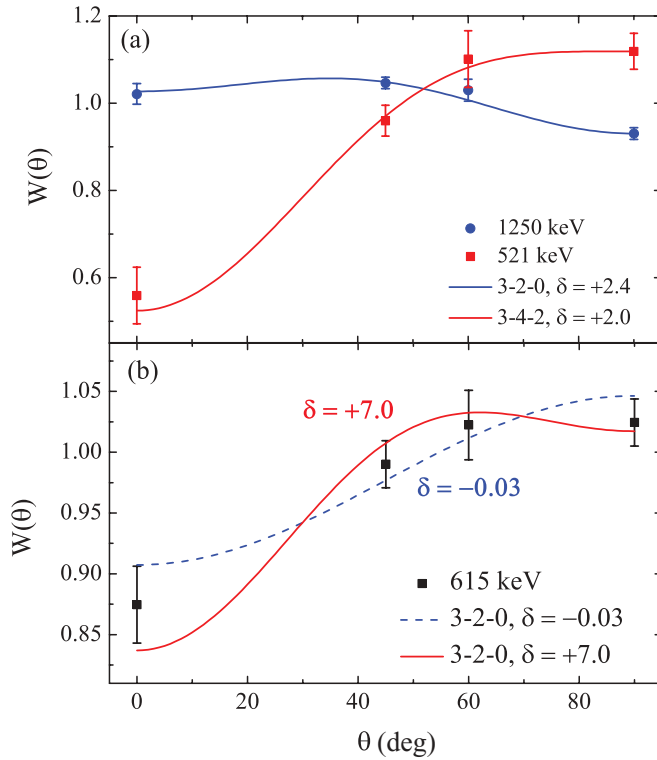


FIG. 5. (Color online) Angular correlation analysis for the transitions depopulating the 3^+ level at 1884 keV, including the (a) 1250- and 521-keV transitions and the (b) 615-keV transition. Symbols indicate the data and the theoretical predictions are represented by lines. The theoretical curves are labeled by the assumed spin sequence and δ value.

the low energy of the 0_2^+ state, its large $E2$ transition strength to the 2_1^+ state, and similarities with states in ^{72}Se . Already, however, Ref. [10] noted some problems with this basic picture in their comparison of $B(E2)$ values predicted by a simple

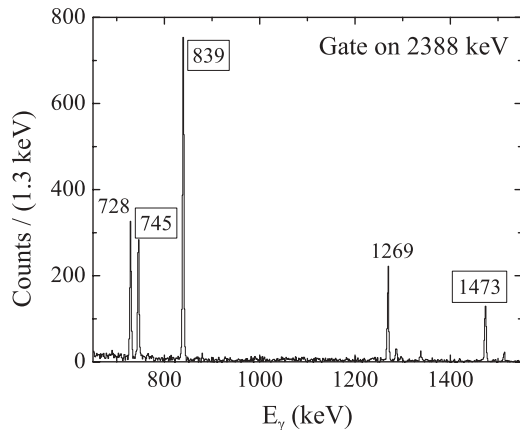


FIG. 6. Spectrum gated on 2388-keV transition providing evidence for a single level at 2108 keV. Transitions are labeled by their energy in keV; those given in boxes are transitions which originate directly from the 2108-keV level, while the others correspond to transitions from levels which are populated in the decay of the 2108-keV level.

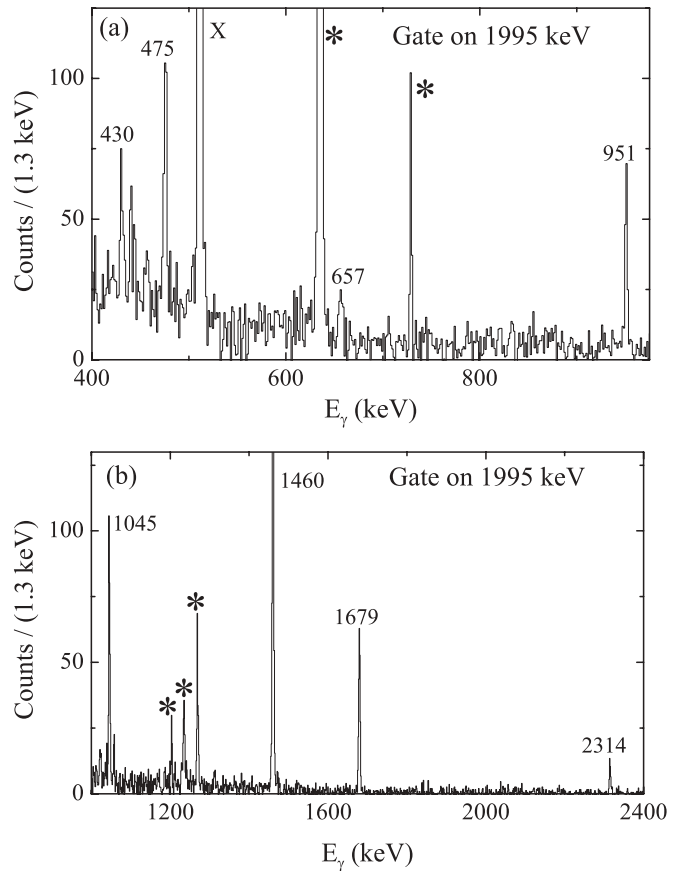


FIG. 7. Spectra gated on the 1995-keV transition providing support for newly observed depopulating transitions from the 2314-keV level. For clarity the spectrum is separated into the energy range (a) 400–1000 keV and (b) 1000–2400 keV. Transitions depopulating the 2314-keV level are indicated by their energy in keV, while decays from subsequent levels are indicated by the (*) symbol. In (a) the 634-/635-keV and 511-keV (indicated by the X symbol) transitions are larger than the y axis scale; similarly in (b) for the 1460-keV transition.

coexistence model to the observed transition strengths. In the present work, the identification of an additional 0^+ state at 1658 keV and newly identified transitions which allow for the calculation of additional $B(E2)$ values casts further doubt on the 0_2^+ level as being the deformed prolate intruder bandhead.

We begin by considering the low-lying structure of ^{74}Se without invoking the notion of shape coexistence. The $R_{4/2} = E(4_1^+)/E(2_1^+)$ of 2.15 is very close to that expected for a spherical vibrator ($R_{4/2} = 2.0$). Furthermore, there are a number of states which seem to follow a multiplet structure expected for a vibrational shape. The 4_1^+ (1363 keV), 2_2^+ (1269 keV), and 0_2^+ (854 keV) levels are usually taken as good candidates for two-phonon states, which would be predicted to lie at approximately $2 \times 635 \text{ keV} = 1270 \text{ keV}$. Such an interpretation agrees nicely with the observed energies of the 2_2^+ and 4_1^+ states; however, obviously the 0_2^+ lies considerably lower than expected for a two-phonon multiplet state. We will return later to an explanation for the energy of the 0_2^+ level. The $B(E2)$ transition strengths also agree well with the predictions for a spherical structure. The level energies and

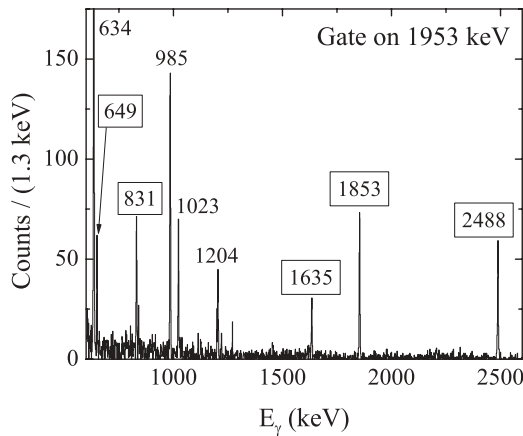


FIG. 8. Spectra gated on the 1953-keV transition providing support for a newly observed level at 2488 keV. Transitions are labeled by their energy in keV; those given in boxes are transitions which originate directly from the 2488-keV level, while the others correspond to transitions from levels which are populated in the decay of the 2488-keV level.

$B(E2)$ strengths are summarized in Fig. 9. Both the $B(E2; 4_1^+ \rightarrow 2_1^+)$ and $B(E2; 0_2^+ \rightarrow 2_1^+)$ strengths are twice that of the $B(E2; 2_1^+ \rightarrow 0_1^+)$ value. The 2_2^+ state shows the expected strong transition strength for the allowed transition to the 2_1^+ state (although a factor of two smaller than that expected for a spherical vibrator) and an almost two-orders-of-magnitude-smaller transition strength to the 0_1^+ state, the latter of which would represent a forbidden transition in the spherical vibrator model.

In the present work, the $2_2^+ \rightarrow 0_2^+$ γ branch is observed for the first time allowing for the determination of $B(E2; 2_2^+ \rightarrow 0_2^+) =$

3.5(11) W.u. This matrix element has significance for understanding the low-lying structure. The corresponding $B(E2)$ strengths in the neighboring nuclei where shape coexistence is known to play a role are significantly larger. In ^{76}Kr , the 2_2^+ and 0_2^+ have been described as both being members of a coexisting deformed intruder band with $B(E2; 2_2^+ \rightarrow 0_2^+) = 157(16)$ W.u. [4]. In ^{72}Se , the 2_2^+ state is also interpreted as the deformed prolate band member but nearly completely mixed with the near spherical 2_1^+ state giving a $B(E2; 2_2^+ \rightarrow 0_2^+)$ of 36(3) W.u. [28]. Now the newly measured $B(E2; 2_2^+ \rightarrow 0_2^+)$ of 3.5(11) W.u. in ^{74}Se indicates that neither state is a member of the deformed rotational band. In contrast, this small value is consistent with an interpretation that both states are members of the two-phonon multiplet.

States belonging to the three-phonon multiplet should lie near 2 MeV. The 6_1^+ (2231 keV), 4_2^+ (2108 keV), and 3_1^+ (1884 keV) are clear candidates. The decays from these states follow phononlike selection rules, as shown in Fig. 9, with a preference for decay to two-phonon states. The $J^\pi = 0^+$ member of this three-phonon multiplet is elusive. The new 0^+ level at 1658 keV may be a candidate. However, if purely vibrational, both the two- and three-phonon 0^+ states would be anomalously low, by ~ 400 keV, without any clear reason. More likely, the three-phonon 0^+ state has yet to be identified, probably near 2 MeV, and the newly assigned state at 1658 keV arises from a prolate deformed intruder configuration. The nonobservation of the three-phonon 0^+ state is not surprising, as this state should be fed in the β decay of the ^{74}Br ground state, which is very weakly populated in the present experiment.

The fact that at high spin the yrast line of ^{74}Se becomes highly prolate collective is not disputed [16], as the larger moment of inertia for the deformed states is strongly favored with spin. The measured $B(E2)$ strengths from the 8^+ , 10^+ , and 12^+ yrast states give an average quadrupole moment of $Q_o \sim 2.3(2)$ eb, consistent with large (prolate) deformation. A fit to the yrast line from $J^\pi = 10^+$ to 18^+ to a simple rotational formula $E = AJ(J+1) + B[J(J+1)]^2$ gives the unperturbed prolate bandhead with $J = 0$ near 1350 keV. Assuming the 1658-keV 0^+ level is the prolate bandhead, mixing between this level and the two-phonon 0^+ level then has perturbed the two states by approximately ± 300 keV. Such a scenario would then imply the unperturbed two-phonon 0^+ energy to be at around 1150 keV, consistent with the energies of the 4^+ and 2^+ proposed members of the multiplet. The perturbed and unperturbed energies then indicate a mixing matrix element of $V \sim 380$ keV and mixing amplitudes such that the lower state is $\sim 60\%$ two-phonon character and $\sim 40\%$ deformed. Such a mixing matrix element is not inconsistent with similar shape coexistence which has been reported for neutron-deficient Kr isotopes where $V = 200\text{--}300$ keV [29].

The situation with high-lying $J = 2$ states is similarly complicated by mixing, with two candidates at 1839 and 2314 keV presumably arising from mixing between the $J = 2$ member of the three-phonon multiplet and the $J = 2$ member of the deformed rotational band. Neither has measured lifetimes to extract absolute $B(E2)$ values; however, we can use relative $B(E2)$ transition strengths to attempt to gain some insight into their structure. The relative $B(E2)$ decays from

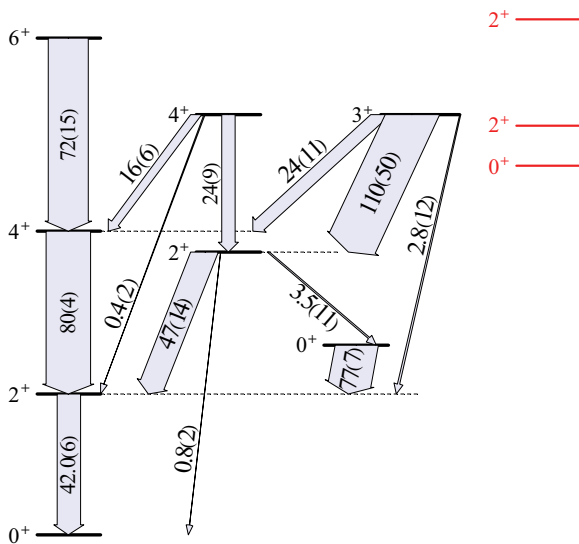


FIG. 9. (Color online) Low-lying levels in ^{74}Se and their γ -decay strengths. Excitation energies are drawn to scale and the widths and labels of the arrow represent the absolute $B(E2)$ transition strengths (in W.u.). The levels in red on the right of the figure are the remaining positive parity levels below 2.4 MeV.

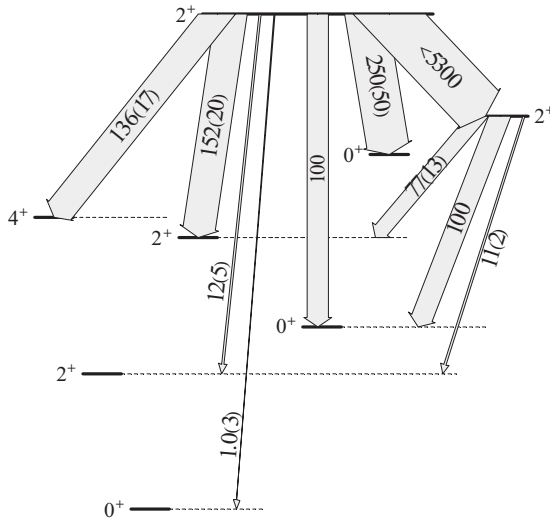


FIG. 10. Decay of the 2_3^+ and 2_4^+ levels in ^{74}Se . Relative $B(E2)$ transition strengths are represented by the width of the arrows and the labels. Those given with limits have unmeasured $E2/M1$ mixing ratios.

the 1839- and 2314-keV levels are given in Fig. 10. From an energy standpoint alone, the 1839-keV level is the better candidate for the 2^+ excitation belonging to the 0_3^+ level. Naturally, one would then expect a transition to the 0_3^+ level. Such a decay is not excluded by our experiment, since the low energy and the E_γ^5 factor makes identification of such a transition difficult. If the $B(E2)$ were 2 times greater than that to the 0_2^+ level, the expected intensity of the γ ray would be on the order of 0.002, an order of magnitude below the sensitivity of the present work.

The decay of the 2_4^+ level is highly fragmented. The decays expected for a member of the three-phonon multiplet are present; strong transitions to the 4_1^+ , 2_2^+ , and 0_2^+ levels and considerably weaker transitions to the 2_1^+ and 0_1^+ levels. However, there is also substantial decay strength to the 0_3^+ and 2_3^+ levels with proposed intruder configurations. The decay to the 0_3^+ level is understandable in the context of complete mixing between the 0_2^+ and 0_3^+ levels. Presumably, the 2_3^+ and 2_4^+ levels also undergo mixing, allowing for a strong transition between the two levels. Assuming the 2_3^+ and 2_4^+ levels are mixed, then in a simple two-level mixing scenario, the transition strength between the levels would be proportional to the difference in quadrupole moments of the two states. While the $2_4^+ \rightarrow 2_3^+$ strength is currently only a limit as the $E2/M1$ mixing ratio is unknown, the large upper limit is consistent with very different deformations for the two states.

B. Strength function and structure

A first glance at Fig. 2 and Table I would suggest an indiscriminate β decay populating many states in ^{74}Se from low to high excitation energy without much selectivity. To investigate the decay of the $J^\pi = 4^{(+)}$ isomer in ^{74}Br , in the following analysis the levels which are clearly populated in the decay of the $J^\pi = (0^-)$ ground state (starred levels in Table I),

and the depopulating γ -ray transitions, are excluded. As mentioned previously, the $J^\pi = (0^-)$ ground state is populated very weakly compared to the $J^\pi = 4^{(+)}$ isomer. For example, γ decays from the (0^-) ground state populate the 2_1^+ level with a total summed intensity of 1.3, compared to the total depopulating intensity of the 2_1^+ level of 100. The levels removed from the present discussion are only those previously identified [20] as originating from the $J^\pi = (0^-)$ ground state. In principle, some of the newly identified levels could also originate from the ground-state decay; however, their impact is most likely $<1\%$ and would not alter significantly the following analysis.

The decay scheme from the $J^\pi = 4^{(+)}$ isomer is normalized assuming that the sum of γ rays and conversion electrons to the ground state is 100, since no ground-state feeding is expected. The β feeding, $I(\epsilon + \beta^+)$, is determined from the difference in normalized γ -ray intensities populating and depopulating each state. Collecting the β -decay feedings into 200-keV bins, as shown in Fig. 11(a), supports a picture of nearly indiscriminate β -decay population, except for some enhancement near 4.5 MeV in excitation energy. To get a clear picture of the relative β -decay matrix elements and the true β strength function, one needs to factor out the Fermi phase-space factor which favors decays to the low-lying states. For example, a squared matrix element to a level at 4.5 MeV needs to be more than 400 times bigger than one at 0.1 MeV in order to result in an equal β branch. When phase space is taken into

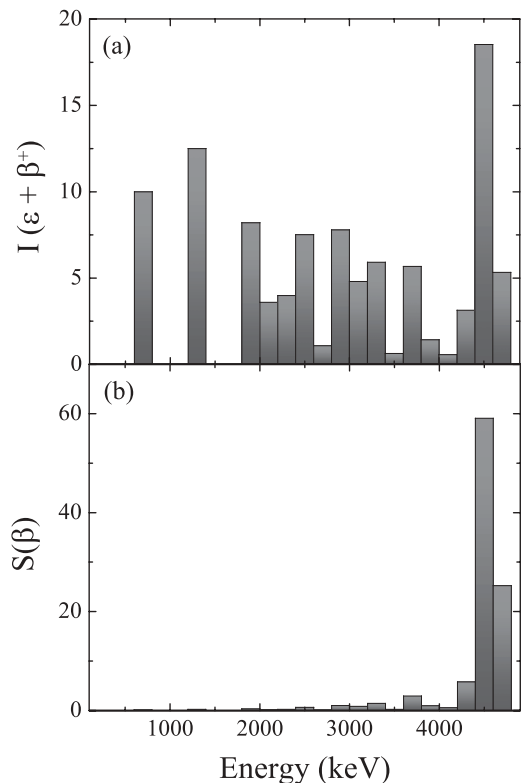


FIG. 11. (a) $\epsilon + \beta^+$ feeding intensities in 200-keV bins. (b) Same as in (a) but the phase-space factor has been divided out to give the decay strength function, $S(\beta)$. All plots are normalized so the total decay strength is 100%.

account, the result is quite striking, as can be seen in Fig. 11(b). The strength function, $S(\beta)$, in Fig. 11(b) is the β feeding intensity divided by the Fermi phase-space factor, which is then normalized such that the total strength is 100. One sees that 59% of the total strength lies in a few states at 4500 ± 100 keV and $>90\%$ in the region 4500 ± 300 keV. The decay Q value for positron emission is $+5906(6)$ keV, yet almost the entire decay selects a mode that only uses 25% of this available energy. Clearly, a special nuclear structure selection is taking place.

To understand this selectivity, one needs to carefully examine the parent state. The dominant ($>90\%$) β decay in this study is not from the ^{74}Br ground state but from the $T_{1/2} = 46$ min, 13.8-keV $J^\pi = 4^{(+)}$ isomer. In-beam spectroscopy indicates that this state is the bandhead for a set of states which are highly deformed and collective in nature with a quadrupole deformation at high spin of $\beta_2 \sim 0.4$ [18]. The large deformation arises from both of the uncoupled valence particles lying in states of $g_{9/2}$ parentage, specifically in the [422]5/2 neutron and [431]3/2 proton Nilsson states. Thus, the β -decay parent is a $J = K = 4$, two-quasiparticle isomer. Similar highly deformed isomers are known in the isotones of ^{74}Br , that is, in ^{76}Rb [30] and in ^{78}Y [31].

Since β decay is described by a single-particle operator, it cannot dramatically alter the collective structure and, consequently, has K -selection rules, as is found for γ decay. The classic case of such a K selection in β decay lies in the rare-earth odd-odd nucleus ^{176}Lu [32], which exhibits a decay from a $J = K = 7$ isomer to members of the $K = 0$ ground state in ^{176}Hf but with $\log ft$ values of >18 . The most favored decay in ^{74}Br is for the valence proton to Fermi decay into a neutron occupying exactly the same Nilsson state, that is, populating a highly deformed $J = K = 4$ two-quasineutron state in ^{74}Se . This configuration lies at quite high excitation energy in selenium, as the low-lying levels of ^{74}Se are near spherical and no prolate states exist below 1.2 MeV. Compared to the lowest-lying state in the deformed minimum, a neutron pair has to be broken (costing ~ 2.5 MeV) then the particles have to be promoted into their “correct” $g_{9/2}$ Nilsson states (involving another 1.0 MeV). Against this, the maximally aligned spin-configuration recoups ~ 0.2 MeV, leaving the $K = 4$ two-quasineutron state at ~ 4.5 MeV. The shape coexistence means the level density of “normal” $J = 4$ states, that is ones of small or no deformation, is quite high so configuration mixing will occur. This is best seen for the pair of states only 6 keV apart at 4586 and 4592 keV. Not only do they receive 8% of the actual decay (30% when corrected for phase space), approximately equally shared, but subsequently they have near-identical γ decays to low-lying states (see Table I), indicative of almost complete mixing.

C. Nonyrast states in the second minimum

Once the $J = K = 4^+$ prolate states in ^{74}Se are populated, their subsequent γ decays are selective and will have large matrix elements to deformed levels nearer to the ground state and favor decay to any high- K states. Again, phase space plays a big role, and while the high-lying states have decay branches to most of the lowest levels, a few special nonyrast

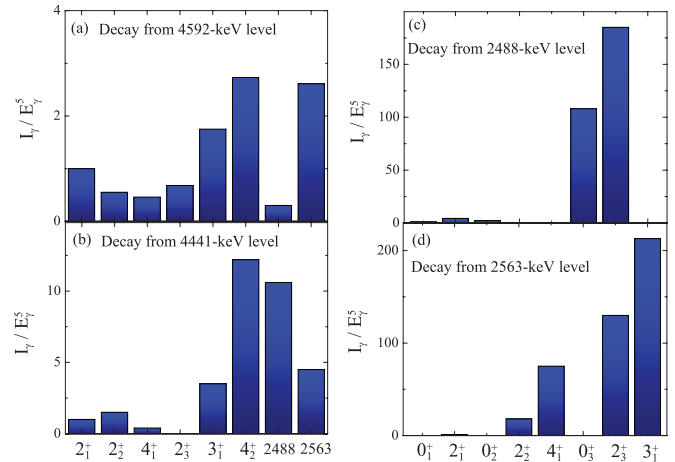


FIG. 12. (Color online) Relative $E2$ decays from the (a) 4496-keV, (b) 4441-keV, (c) 2488-keV, and (d) 2563-keV levels. (a), (b), and (d) are normalized such that the decay to the 2_1^+ level is 1.0, whereas (c) is normalized to 1.0 for decay to the 0_2^+ level. All transitions are assumed to be $E2$ in character.

states are populated with relatively large matrix elements and consistently high branches. Figures 12(a) and 12(b) show the phase-space-corrected (E_γ^5) $E2$ matrix elements between some of the states that are strongly populated in β decay and lower-lying structures. Such a selective decay can be a tool for separating the prolate-deformed and spherical states. For example, in the deformed minimum one should expect a “quasi- γ -vibrational band,” a ubiquitous feature of even-even deformed nuclei in this region. Pure γ bands in rigid axial nuclei have $K = 2$. In the $A \sim 80$ region, though, there is considerable γ softness, as evidenced by the odd-spin, even-spin staggering in all these γ bands, so it is not clear how rigorously the spin projection is preserved. Nonetheless, for a parent state with $K = 4$, one would expect a decay which will favor the γ band or any other high- K structures. In the decay of the strongly populated states around 4.4–4.6 MeV, the levels at 2488 and 2563 keV are frequently populated with considerable transition strengths in some cases, with examples of the decays of a few states shown in Figs. 12(a) and 12(b). The subsequent decay of these 2488- and 2563-keV levels is given in Figs. 12(c) and 12(d). The decay from these levels clearly favors population of the 1658-keV and 1839-keV levels, which we have identified as the candidates for the first members of the prolate-deformed ground-state band, albeit quite mixed with vibrational states. This pattern of γ decay is what one would expect from the $J = 2$ and $J = 3$ states in the γ band.

IV. CONCLUSIONS

We have re-examined the β decay of ^{74}Br populated following the $^{60}\text{Ni}(^{16}\text{O}, pn)$ reaction which favored population of the $J = K = 4$ β -decaying isomer at 13.8 keV. Using a large modern array of γ detectors, we were able to extend and correct the decay scheme and constrain many spins, parities, and mixing ratios in ^{74}Se , including identifying a new $J = 0_3^+$ state at 1658 keV. The new decay scheme

helps clarify the shape coexistence as between near spherical and prolate deformed, with an unperturbed prolate bandhead close to 1350 keV. The unusual β -decay parent state is very deformed with $K = 4$ and so has a very selective β decay with large matrix elements to levels in ^{74}Se near 4.5 MeV, presumably a two-quasineutron configuration based on $g_{9/2}$ particles. In turn, these states are selective in their γ decay and favor the low-lying prolate configurations. The selectivity suggests candidates for a $K = 2$ quasi- γ band at ~ 1300 keV excitation in the second minimum, an interesting and unusual feature.

ACKNOWLEDGMENTS

This work was supported by the DOE Office of Nuclear Physics under Contracts No. DE-AC02-06CH11357 and No. DE-AC02-98CH10946, Grants No. DE-FG02-94ER40848 and No. DE-FG02-91ER40609, and by Deutsche Forschungsgemeinschaft under Contracts No. ZI S10/4-1 and No. SFB 634. M.E. was supported by the Bonn-Cologne Graduate School of Physics and Astronomy. D.S. and D.R. acknowledge support from the German Academic Exchange Service (DAAD). The authors are grateful to the WNSL technical staff for their skillful operation of the tandem.

-
- [1] R. V. F. Janssens and T. L. Khoo, *Ann. Rev. Nucl. Part. Sci.* **41**, 321 (1991).
- [2] V. Metag, D. Habs, and H. J. Specht, *Phys. Rep.* **65**, 1 (1980).
- [3] S. Nummela *et al.*, *Phys. Rev. C* **64**, 054313 (2001).
- [4] E. Clément *et al.*, *Phys. Rev. C* **75**, 054313 (2007).
- [5] J. Ljungvall *et al.*, *Phys. Rev. Lett.* **100**, 102502 (2008).
- [6] C. Plettner *et al.*, *Phys. Rev. Lett.* **85**, 2454 (2000).
- [7] A. Petrovici, K. W. Schmid, and A. Faessler, *Nucl. Phys. A* **605**, 290 (1996).
- [8] M. Bender, P. Bonche, and P.-H. Heenen, *Phys. Rev. C* **74**, 024312 (2006).
- [9] M. Girod, J.-P. Delaroche, A. Görgen, and A. Obertelli, *Phys. Lett. B* **676**, 39 (2009).
- [10] R. M. Ronningen, A. V. Ramayya, J. H. Hamilton, W. Lourens, J. Lange, H. K. Carter, and R. O. Sayer, *Nucl. Phys. A* **261**, 439 (1976).
- [11] R. B. Piercey, A. V. Ramayya, R. M. Ronningen, J. H. Hamilton, V. Maruhn-Rezwani, R. L. Robinson, and H. J. Kim, *Phys. Rev. C* **19**, 1344 (1979).
- [12] J. Adam, M. Honusek, A. Špalek, D. N. Doynikov, A. D. Efimov, M. F. Kudojarov, I. Kh. Lemberg, A. A. Pasternak, O. K. Vorov, and U. Y. Zhovliev, *Z. Phys. A* **332**, 143 (1989).
- [13] F. S. Radhi and N. M. Stewart, *Z. Phys. A* **356**, 145 (1996).
- [14] A. Algora, T. Fényes, Zs. Dombrádi, and J. Jolie, *Z. Phys. A* **352**, 25 (1995).
- [15] P. D. Cottle, J. W. Holcomb, T. D. Johnson, K. A. Stuckey, S. L. Tabor, P. C. Womble, S. G. Buccino, and F. E. Durham, *Phys. Rev. C* **42**, 1254 (1990).
- [16] J. Döring, G. D. Johns, M. A. Riley, S. L. Tabor, Y. Sun, and J. A. Sheikh, *Phys. Rev. C* **57**, 2912 (1998).
- [17] G. Winter, J. Döring, W. D. Fromm, L. Funke, P. Kemnitz, and E. Will, *Z. Phys. A* **309**, 243 (1983).
- [18] J. W. Holcomb, T. D. Johnson, P. C. Womble, P. D. Cottle, S. L. Tabor, F. E. Durham, and S. G. Buccino, *Phys. Rev. C* **43**, 470 (1991).
- [19] B. Singh and A. R. Farhan, *Nucl. Data Sheets* **107**, 1923 (2006).
- [20] H. Schmeing, R. L. Graham, J. C. Hardy, and J. S. Geiger, *Nucl. Phys. A* **233**, 63 (1974).
- [21] A. Coban, J. C. Lisle, G. Murray, and J. C. Willmott, *Part. Nucl.* **4**, 108 (1972).
- [22] S. Göring and M. v. Hartrott, *Nucl. Phys. A* **152**, 241 (1970).
- [23] B. Singh, *Nucl. Data Sheets* **101**, 193 (2004).
- [24] K. Abusaleem and B. Singh, *Nucl. Data Sheets* **112**, 133 (2011).
- [25] K. S. Krane and R. M. Steffen, *Phys. Rev. C* **2**, 724 (1970).
- [26] C. G. Barham, S. S. Alghamdi, A. Bhagwat, M. Booth, I. S. Grant, M. Lindroos, J. Rikowska, B. D. D. Singleton, N. J. Stone, and P. M. Walker, *Hyperfine Interact.* **75**, 433 (1992).
- [27] M. Borsaru, D. W. Gebbie, J. Nurzynski, C. L. Hollas, L. O. Barbopoulos, and A. R. Quinon, *Nucl. Phys. A* **284**, 379 (1977).
- [28] E. A. McCutchan, C. J. Lister, T. Ahn, R. J. Casperson, A. Heinz, G. Ilie, J. Qian, E. Williams, R. Winkler, and V. Werner, *Phys. Rev. C* **83**, 024310 (2011).
- [29] E. Bouchez *et al.*, *Phys. Rev. Lett.* **90**, 082502 (2003).
- [30] D. Rudolph *et al.*, *Phys. Rev. Lett.* **76**, 376 (1996).
- [31] J. Uusitalo *et al.*, *Phys. Rev. C* **57**, 2259 (1998).
- [32] J. Arnold, *Phys. Rev.* **93**, 743 (1954).